TUP-Springer Project

[罗马尼亚] Nicolae M. Avram
[爱沙尼亚] Mikhail G. Brik
Editors

晶体中3d离子的光学性质
光谱和晶场分析

Optical Properties of 3d-Ions in Crystals
Spectroscopy and Crystal Field Analysis

清华大学出版社
Springer

Nicolae M. Avram
Mikhail G. Brik

晶体中3d离子的光学性质：光谱和晶场分析

Optical Properties of 3d-Ions in Crystals: Spectroscopy and Crystal Field Analysis

内容简介

The book is devoted to the analysis of spectral, vibronic and magnetic properties of 3d ions in a wide range of crystals, used as active media for solid state lasers and potential candidates for this role. Crystal field calculations (including first-principles calculations of energy levels and absorption spectra) and comparison of these results with experimental spectra, Janh-Teller effect, analysis of vibronic spectra, materials science applications are systematically dealt with. The chapters are relatively independent and can be read separately.

The book can be useful for researchers working in the areas of crystal spectroscopy, materials science and its optical applications, post-graduate and under graduate students.

图书在版编目(CIP)数据

晶体中 3d 离子的光学性质: 光谱和晶场分析 = Optical Properties of 3d-Ions in Crystals: Spectroscopy and Crystal Field Analysis: 英文/(罗马尼亚)阿弗莱(Avram, N. M.),(爱沙尼亚)布莱克(Brik, M. G.)著. --北京：清华大学出版社，2012.12

ISBN 978-7-302-28545-8

Ⅰ.①晶… Ⅱ.①阿… ②布… Ⅲ.①离子光学-研究-英文 Ⅳ.①O463

中国版本图书馆 CIP 数据核字(2012)第 072851 号

责任编辑：陈朝晖
责任校对：赵丽敏
责任印制：李红英

出版发行：清华大学出版社
网　址：http://www.tup.com.cn，http://www.wqbook.com
地　址：北京清华大学学研大厦 A 座　　邮　编：100084
社总机：010-62770175　　邮　购：010-62786544
投稿与读者服务：010-62776969，c-service@tup.tsinghua.edu.cn
质　量　反　馈：010-62772015，zhiliang@tup.tsinghua.edu.cn
印 装 者：北京雅昌彩色印刷有限公司
经　　销：全国新华书店
开　　本：153mm×235mm　　**印　张**：17.5　　**字　数**：395 千字
版　　次：2012 年 12 月第 1 版　　**印　次**：2012 年 12 月第1 次印刷
印　　数：1～1000
定　　价：88.00 元

产品编号：030713-01

List of contributors

C.N. Avram
Department of Physics, West University of Timisoara,
Bd. V. Parvan No.4, 300223 Timisoara, Romania
Phone: +40-256-592187; Fax: +40-256-592108
E-mail: acalin@physics.uvt.ro

N.M. Avram
Department of Physics, West University of Timisoara,
Bd. V. Parvan No.4, 300223 Timisoara, Romania.
Phone: +40-256-592187; Fax: +40-256-592108
and
Academy of Romanian Scientists, Splaiul
Independentei 54, 050094-Bucharest, Romania
E-mail: avram@physics.uvt.ro

G. Bevilacqua
CNSIM and Dipartimento di Fisica, Universita' di Siena,
Via Roma 56, I-53100 Siena, Italy
Phone: +39-0577-234682; Fax: +39-0577-234689
E-mail: bevilacqua@unisi.it

M.G. Brik
Institute of Physics, University of Tartu, Riia 142,
Tartu 51014, Estonia.
Phone: +372-7374751; Fax: +372-7383033
E-mail: brik@fi.tartu.ee

I.V. Kityk
Electrical Engineering Department, Czestochowa Technological
University, Al. Armii Krajowej 17/19, Czestochowa, Poland
E-mail: kityk@wp.pl

S. Kück
Physikalisch-Technische Bundesanstalt AG 4.13
Laserradiometrie, Bundesallee 100,
38116 Braunschweig,Germany
Phone: +49-531592-4111, -4141
Fax: +49-531592-4105, -4116, -694111
E-mail: stefan.kueck@ptb.de

L. Martinelli — Dipartimento di Fisica "Enrico Fermi", Universita' di Pisa, Largo B. Pontecorvo 3, I-56127 Pisa, Italy
Phone: +39-050-2214846, Fax: +39-050-2214333
E-mail: liana.martinelli@df.unipi.it

E.E. Vogel — Departamento de Ciencias Fisicas, Universidad de la Frontera, Casilla (P.O. Box) 54-D, Avenida Francisco Salazar 0115, Temuco, Chile
Phone: +56-45-325316; Fax: +56-45-325323
E-mail: ee_vogel@ufro.cl

Y.Y. Yeung — Department of Mathematics, Science, Social Sciences and Technology, The Hong Kong Institute of Education, 10 Lo Ping Road, Tai Po, New Territories, Hong Kong SAR, People's Republic of China
Phone: +852-29487650; Fax: +852-29487676
Email: yyyeung@ied.edu.hk

W.C. Zheng — Department of Material Science,Sichuan University, Wangjiang Road 29, Chengdu 610064, People's Republic of China
Phone: +862-885412371; Fax: +862-885416050
E-mail: zhengwc1@163.com

Contents

1 Recent development in laser crystals with 3d ions

S. Kück

Physikalisch-Technische Bundesanstalt AG 4.13 Laserradiometrie, Bundesallee 100
38116 Braunschweig, Germany

Abstract This chapter will give an overview about the recent advances on the fieldof lasers, based on the 3d ions. The main focus is set on the lasercharacteristics and results obtained within the last few years.In general, transition metals are elements of the 3rd, 4th and 5th row in the periodictable. However, laser oscillation was only obtained thus far mainly withions of transition metals of the 3rd row (Fe-row, Ti to Cu); therefore, thefocus of this chapter is on these ions. The outstanding characteristics ofthese ions i.e. their broad band emission, is caused by the fact that theirelectronic levels couple strongly to the surrounding field which isestablished by the crystalline environment, forming the so called vibronic levels. Therefore, transition metal ion lasers usually are tunable over a widespectral range up to several to hundreds of nanometers, making theminteresting sources for frequency comb generation, short pulse generationas well as for applications in many scientific fields, were coherenttunable laser radiation is essential.

Keywords Tunable solid state lasers; transition metal ion lasers; transition metal ion spectroscopy; absorption, excitation, emission, luminescence; electroluminescence; emission lifetimes; nonradioactive decay; multiphonon relaxation; quantum efficiency; excited state absorption; laser materials; vibronic transitions; phonon coupling; 4-level lasers; near-infrared lasers; mid-infrared lasers; room temperature lasers; continuous wave lasers; mode locking; short pulse generation; femtosecond lasers; crystal and ligand fields; ligand coordination.

1.1 Introduction

This chapter will give an overview about the recent advances on the field of lasers, based on 3d ions. The main focus is set on the laser characteristics and results obtained within the last few years. A detailed overview on transition metal lasers since the beginning of laser operation is given in [1], a more spectroscopically oriented overview is given in [2]. In general, transition metals are elements of 3rd,

4th and 5th row in the periodic table. However, laser oscillation was only obtained thus far with ions of transition metals of the 3rd row (Fe-row, Ti to Cu), therefore, the focus of this chapter is on these ions. The outstanding characteristics of these ions i.e. their broad band emission, is caused by the fact that their electronic levels couple strongly to the surrounding field which is established by the crystalline environment, forming vibronic levels. Therefore, *transition metal ion lasers* usually are tunable over a wide spectral range up to several to hundreds of nanometers.

Right after the demonstration of the Ruby ($Cr^{3+}Al_2O_3$) laser in 1960 [3] a number of crystalline and glass lasers were realized within the following decade, however, mainly based on divalent or trivalent rare earth ions. It was in the end of the 70ties and the beginning of the 80ties, when successful and efficient laser operation of Cr^{3+}-doped [4-7] and Ti^{3+}-doped crystals [8, 9] were achieved. These tunable *room temperature lasers* have stimulated further research in transition metal ions as active ions in crystals. Interesting new results with respect to application and efficiency have been obtained with the Cr^{4+}-ion [10-13] at the beginning of the 90ties and with the divalent Cr^{2+}-ion [14] in the mid 90tie.

The applications of *transition metal ion lasers* is predominantly in those fields, where the tunability is of outstanding characteristic, i.e. to produce ultra short pulses via mode-locking, for applications, where the wavelength has to be exactly adjusted e.g. to a specific transition of an atom, ion, and molecule which is under investigation or where the coherence occurs and thus brilliance over a wide spectral range is required. Such applications are used in scientific research, medicine, measurement and testing techniques, ultra short pulse generation, communication and very recently in photometry [15]. Via second harmonic generation, optical parametric oscillation, and sum- and difference-frequency generation the tunability can be transferred into other spectral regions which are not accessible via tunable lasers operating on the fundamental wavelength. *Transition metal ion lasers* are not supposed to be competitors to high power/high energy lasers, as e.g. Yb^{3+} and Nd^{3+} lasers.

The outline of this chapter is as follows: After this introductory section, a brief introduction into the general properties of *transition metal ion lasers* will be given in section 2. In the third section, the recent progress on the field of the transition metal ion doped laser materials will be given. Finally, a summary and an outlook for transition metal ions will be given.

1.2 General properties and aspects of tunable solid-state lasers

In general, for the understanding and description of the lasers based on transition metal ions, several different aspects have to be taken into account. These aspects concerning preparation, spectroscopy and laser operation were thoroughly discussed in the overview articles [1, 2] and the appropriate literate cited therein. Thus,

they will be only briefly presented here. Greater focus, however, is laid on the temperature dependence of the lifetime and the *excited state absorption*, which are the main parameters and characteristics determining the laser behavior of a transition metal ion doped system.

1.2.1 The prep rational aspect

The Prep rational aspects are as follows:

1. Transition metal ions usually occurs in several valence state as well as in different kinds of co-ordinations of the surrounding first shell of ligands, i.e. tetrahedral (4), octahedral (6), and cubic (8). Both characteristics determine strongly the energy level scheme of a transition metal ion.
2. The coordination number and the site symmetry determine the transition selection rules. Thus, usually transitions for ions in the tetrahedral co-ordination are much stronger than transitions for ions in the octahedral coordination, because of the lack of a center of inversion in the case of tetrahedral coordination.
3. The valence of an ion determines the spectroscopic properties and eventually the laser characteristics.
4. The crystal quality directly affects the laser efficiency.

1.2.2 The spectroscopic aspect

The energy level schemes of the transition metal ions in crystalline hosts are in principle described by the so called Tanabe-Sugano diagrams [16-18]. These diagrams are distinguished by the number of electrons within the 3d-electron shell. In these diagrams the energy of a specific level of the transition metal ion is depicted as a function of the crystal field strength. We will not describe the quantum mechanical background needed to obtain these diagrams; this would be beyond the frame of this chapter. The reader is referred to appropriate literature [19-24]. The investigation of a transition metal ion doped crystal with respect to its possible laser characteristics which includes the determination of all laser relevant parameters by spectroscopic methods. The basic measurements are the ground state absorption, the spontaneous emission cross sections and lifetimes and the excitation spectrum, see [1, 2].

1.2.2.1 Emission lifetime and its temperature dependence

The lifetime of an excited state of a transition metal ion usually is temperature dependent. The temperature dependence can be described partly by the model of Struck & Fonger [25] using the so-called Single Configuration Coordinate Model, which describes the interaction between the electronic center and the vibrating crystalline environment. This model describes the radioactive and the nonradioactive

transitions between the two vibronic levels u_n and v_m. The transition probability is proportional to the square of the overlap integral $\langle u_n \mid v_m \rangle$, where u_n and v_m describe the vibronic wave functions of the ground state and the excited state. In case of parabolic potentials (harmonic approximation), these are wave functions of a harmonic oscillator. For the case of a radioactive transition between the v and u states, a photon of energy $\hbar v$ will be emitted. In nonradioactive decay there is none or only a very small difference between the u_n and v_m levels. Therefore, a direct "tunneling process" exists between the two levels, followed by a relaxation into the lower vibronic levels. In thermal equilibrium, the population of the vibronic level within each electronic state will follow the Boltzmann statistics. The following transition probabilities for the radioactive and the nonradioactive rate are determined:

$$\text{Radioactive: } R_{nm} = R_{uv}(1 - r_v)r_v^m \mid \langle u_n \mid v_m \rangle \mid^2, \tag{1.1}$$

$$\text{Nonradioactive: } N_{nm} = R_{ur}(1 - r_v)r_v^m \mid \langle u_n \mid v_m \rangle \mid, \tag{1.2}$$

where the electronic factor $R_{uv} = 10^2$ Hz (forbidden transitions)-10^9 Hz (allowed transitions), $R_{ur} = 10^{12}$ Hz-10^{14} Hz, is the thermal population of photonic level m in the $(1 - r_v)r_v^m$ electronic level v, and nd $r_v = \exp(-\hbar\omega / kT)$.

Thus, the transition rates R_{nm} and N_{nm} differ only due to the electronic factors R_{uv} and R_{nr}. The total rates W_r and W_{nr} for the radioactive and nonradioactive decay, respectively, are determined by summations. The total radioactive rate W_r results from a summation over all the transitions between the electronic levels v and u:

$$W_r = \sum_{n,m} R_{nm} = \sum_{n,m} R_{uv}(1 - r_v)r_v^m \mid \langle u_n \mid v_m \rangle \mid^2 = R_{uv} \tag{1.3}$$

Thus, the radioactive rate within the Struck and Fonger model is independent from the temperature. It does not take into account the coupling of the parity-breaking phonons, see below.

For the calculation of the nonradioactive rate the summation is carried only over the levels u_n and v_m having the same energy, because only in that case the tunnel-ing process can take place. At higher temperature however, the higher phonon (or vibrational) levels are populated, thus the nonradioactive rate increases with temperature. For simplification, within the model of Struck and Fonger only phonons with an effective energy $\hbar / \text{eff}$ will be considered, thus:

$$n\hbar / u - m\hbar / v = p\hbar / \text{eff}, \tag{1.4}$$

where $\hbar / u$ and $\hbar / v$ are the phonon energies in the ground and in the excited state, respectively. The value of p results from the zero phonon energy of the transition:

$$p\hbar / \text{eff} = h\nu_{zp} \tag{1.5}$$

The total nonradioactive rate is:

$$W_{nr} = \sum_{m=0} N_{nm} = \sum_{m=0}^{\infty} R_{nr}(1-r_v) r_v^m \mid \langle u_n \mid v_m \rangle \mid^2 = R_{nr} U_p, \tag{1.6}$$

where

$$U_p = \sum_{m=0}^{\infty} (1-r_v) r_v^m \mid \langle u_n \mid v_m \rangle \mid^2 \tag{1.7}$$

In this sum m and n are connected according to Eq. (1.4). For the U_p the following condition holds true:

$$\sum_p U_p = 1 \tag{1.8}$$

The calculation of the U_p is possible with the help of the Manneback equations [26]. In case of equal force constants in the ground and the excited states (which is equivalent to identical curvatures of the potential energy parabolas of both states), the U_p are simplified to the Huang-Rhys-Pekar-W_p functions, which are defined by the following recursive equation:

$$S_0 \langle m \rangle W_{p+1} + p W_p - S_0 \langle 1+m \rangle W_{p-1} = 0 \tag{1.9}$$

where S_0 is the Huang-Rhys-Pekar factor, and

$$\langle m \rangle = [\exp(\hbar\omega / kT) - 1]^{-1} \tag{1.10}$$

$$\sum_p W_p = 1 \tag{1.11}$$

The exact solution for the W_p is:

$$W_p = \exp(-S_0 \langle 2m+1 \rangle) \sum_{j=0}^{\infty} \frac{S_0 \langle m \rangle^j (S_0 \langle 1+m \rangle)^{p+j}}{j!(p+j)!} \tag{1.12}$$

In the Stirling approximation this can be further simplified to:

$$W_p = \exp(-S_0 \langle 2m+1 \rangle) \frac{\exp(p^*)}{\sqrt{2\pi p^*}} \left(\frac{2 S_0 \langle 1+m \rangle}{p+p^*} \right)^2 \tag{1.13}$$

where $p^* = \sqrt{p^2 + 4 S_0^2 \langle 1+m \rangle \langle m \rangle}$, $\langle m \rangle = \dfrac{r}{1-r} = \dfrac{1}{\exp(\hbar\omega / kT) - 1}$, $r = \exp(\hbar\omega / kT)$

The approximation is valid for $p^* > 1$. For $T = 0$ K Eq. (1.13) gives the

nonradioactive rate $W_{nr}(0)$:

$$W_{nr}(0) = R_{nr}\frac{\exp(p-S)}{\sqrt{2\pi p}}\left(\frac{S}{p}\right)^{p} \tag{1.14}$$

In Fig. 1.1 the nonradioactive rate $W_{nr}(0)$ as a function of the number of effective phonons for different values of the Huang-Rhys-Pekar factor S is shown; R_{nr} was set to 10^{14} Hz. As expected, high values for the nonradioactive rate are present for high values of S and p. With increasing number of phonons and decreasing value of S the nonradioactive rate decreases and leads to the Kiel-multi phonon law, see section 0.

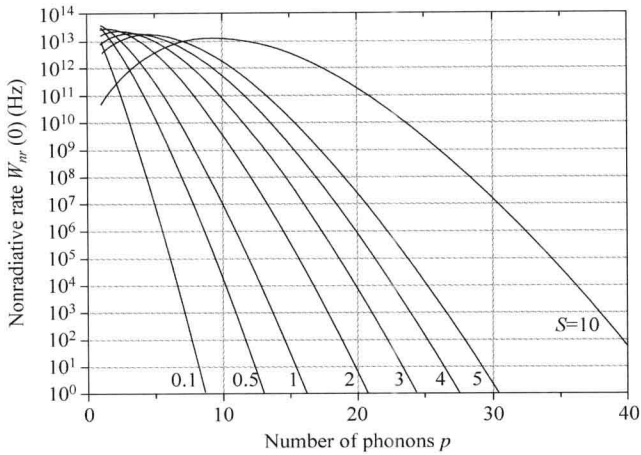

Figure 1.1 Nonradioactive decay rate $W_{nr}(0)$ for different values of S as function of the number of phonons p

With Eqs. (1.14) and (1.13) for the total nonradioactive decay rate can be transformed into a very concise format, which can be used for fitting temperature dependent lifetime data:

$$W_{nr}(T) = W_{nr}(0)\sqrt{\frac{p}{p^*}}\left(\frac{2p\langle 1+m\rangle}{p+p^*}\right)^{p}\exp(p^*-p-2mS). \tag{1.15}$$

The origin of the temperature dependence of the radioactive rate is the coupling of parity-breaking i.e. in general non-centrosymmetric (odd), phonons with the transition. This enhances the transition probability, because the prohibition weakens due to the mixing of levels with different parity via these odd parity phonons. At higher temperatures, the phonon levels of these parity-breaking phonons will be higher populated, thus the radioactive rate increases. The effect can be described

by the Coth-law, which takes into account the phonon occupation [19]:

$$W_r(T) = \frac{1}{\tau(T)} = \frac{1}{\tau_r(0)} \coth\left(\frac{\hbar\omega_{\text{vib}}}{2kT}\right), \tag{1.16}$$

with $\tau(T)$ and $\tau_r(0)$ being the radioactive lifetimes at temperature T and $T=0$ K, respectively, and $\hbar\omega_{\text{vib}}$ being the energy of the odd-parity phonon.

The total decay rate and its temperature dependence can now be calculated from the above derived equations, for the temperature dependence of the radioactive and nonradioactive rate:

$$\begin{aligned} W(T) &= W_r(T) + W_{nr}(T) = W_r(\tau_r, \hbar\omega_{\text{vib}}) + W_{nr}(R_{nr}, \hbar\omega, S, p) \\ &= \frac{1}{\tau_r(0)} \coth\left(\frac{\hbar\omega_{\text{vib}}}{2kT}\right) + W_{nr}(0) \sqrt{\frac{p}{p^*}} \left(\frac{2p\langle 1+m\rangle}{p+p^*}\right)^p \exp(p^* - p - 2mS) \end{aligned} \tag{1.17}$$

The temperature dependent *quantum efficiency* can be determined from:

$$\eta(T) = \frac{W_r(T)}{W(T)} = \frac{\tau(T)}{\tau_r(T)} \tag{1.18}$$

It should be noted that Eq. (1.17) contains 6 independent variables, so that one should be careful to use this equation for fitting without having enough knowledge about the different parameters e.g. for spectroscopy. However, the equation was very successfully used e.g. for the fit of the temperature dependent lifetime of 1) Cr^{4+}-doped [27] and, 2) Mn^{3+}-doped garnet crystals [28]. Here, a series of different garnets crystals were analyzed with the same or nearly the same site symmetry for the Cr^{4+} ion, so that the fitted parameters were only marginally changed for the different host materials.

Borderline cases for the nonradioactive rate

Two borderline cases of the Struck and Fonger model should be mentioned here, 1) the Mott activation energy model [29] and, 2) the multi-phonon-law from Kiel [30]. For large values of S and small values of $W_{nr}(0)$, the nonradioactive decay rate can be described by the activation energy model of Mott. It assumes a thermal population in the excited state, which yields a photonic relaxation at the crossing points of the ground and excited state parabola. The nonradioactive can be expressed as:

$$W_{nr}(T) = A_m \exp\left(-\frac{E_x}{kT}\right), \tag{1.19}$$

where A_m is a constant of about 10^{13} Hz, and E_x is the activation energy, i.e. the energy between the minimum of the excited state parabola an the crossing point with the ground state parabola.

The values for A_m and E_x are difficult to determine experimentally, E_x can be approximated from the zero phonon energy and the Huang-Rhys-parameter S. However, due to the exponential factor, the model always yields $W_{nr}(T=0)=0$.

For small values of the Huang-Rhys parameter S as in the case of the 4f-4f transitions of the trivalent rare earth ions, the multi-phonon-law of Kiel is often used for the description of the temperature nonradioactive decay rate:

$$W_{nr}(T) = A_k \varepsilon^p (1 + \langle m \rangle_v)^p, \tag{1.20}$$

where A_k is a constant, ε is a coupling constant, p stands for the number of photons is the bridging gap between excited state and ground state, and $\langle m \rangle v$ is thermal population of the excited state.

1.2.2.2 Excited state absorption (ESA)

The *excited state absorption* is one of the most decisive factors affecting the laser performance of the transition metal ion doped laser materials where in some cases it even prohibits laser oscillation at all. Therefore the knowledge of its cross sections at the pump and at the laser wavelength (see Fig. 1.2) is of importance for the understanding of the observed laser behavior and efficiency. Furthermore, the measurements of the *excited state absorption* might give a more detailed insight of energy level structure of an ion. Especially transitions into higher lying levels, which are hidden within the band-band transition of the host, might be observable in the ESA spectrum because the transition between the level of meta-stable and the higher lying occurs in this case at energies below the band-band transition. Also, due to the interconfigurational transition, the spin-flip transition often cannot be observed in the ground state absorption spectrum, especially if they are hidden under a spin-allowed transition or are spectrally broad. If the meta-stable level has a different spin state than the ground state (e.g. Cr^{3+} in strong crystal fields, Mn^{5+} [31], Fe^{6+}) the ESA spectrum reveals the transition from the meta-stable state to the states with the same spin. Hence, the crystal field parameters are often determined with higher accuracy. The third aspect of ESA, i.e. its usage as part of an efficient up conversion pump process as in the case of e.g. Er^{3+} visible lasers [1], is not of any importance for *transition metal ion lasers*, because only a few transition metal ions exhibit emission from other levels than the first excited state.

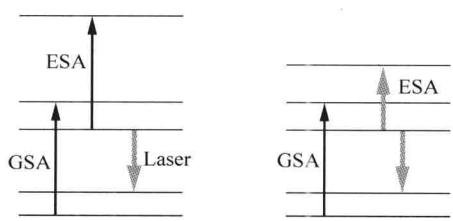

Figure 1.2 Left: *Excited state absorption* on the pump wavelength, right: *Excited state absorption* on the laser wavelength